

Plastic deformation mechanism transition of Ti/Ni nanolaminate with pre-existing crack: Molecular dynamics study

Meng-Jia Su(宿梦嘉), Qiong Deng(邓琼), Min-Rong An(安敏荣), Lan-Ting Liu(刘兰亭)

Citation: Chin. Phys. B . 2020, 29(11): 116201 . **doi:** 10.1088/1674-1056/aba2e5
Journal homepage: http://cpb.iphy.ac.cn; http://iopscience.iop.org/cpb

What follows is a list of articles you may be interested in

Balancing strength and plasticity of dual-phase amorphous/crystalline nanostructured Mg alloys

Jia-Yi Wang(王佳怡), Hai-Yang Song(宋海洋), Min-Rong An(安敏荣), Qiong Deng(邓琼), Yu-Long Li(李玉龙)

Chin. Phys. B . 2020, 29(6): 066201 . **doi:** 10.1088/1674-1056/ab84d5

Anisotropic plasticity of nanocrystalline Ti: A molecular dynamics simulation

Minrong An(安敏荣), Mengjia Su(宿梦嘉), Qiong Deng(邓琼), Haiyang Song(宋海洋), Chen Wang(王晨), Yu Shang(尚玉)

Chin. Phys. B . 2020, 29(4): 046201 . **doi:** 10.1088/1674-1056/ab7188

Investigation of mechanical properties of twin gold crystal nanowires under uniaxial load by molecular dynamics method

Guo-Wei Zhang(张国伟), Zai-Lin Yang(杨在林), Gang Luo(罗刚)

Chin. Phys. B . 2016, 25(8): 086203 . **doi:** 10.1088/1674-1056/25/8/086203

ReaxFF molecular dynamics study on oxidationbehavior of 3C-SiC: Polar face effects

Sun Yu, Liu Yi-Jun, Xu Fei

Chin. Phys. B . 2015, 24(9): 096203 . **doi:** 10.1088/1674-1056/24/9/096203

Effects of tilt interface boundary on mechanical properties of Cu/Ni nanoscale metallic multilayer composites

Yang Meng, Xu Jian-Gang, Song Hai-Yang, Zhang Yun-Guang

Chin. Phys. B . 2015, 24(9): 096202 . **doi:** 10.1088/1674-1056/24/9/096202

Plastic deformation mechanism transition of Ti/Ni nanolaminate with pre-existing crack: Molecular dynamics study*

Meng-Jia Su(宿梦嘉)[1,2], Qiong Deng(邓琼)[1,2,†], Min-Rong An(安敏荣)[3,‡], and Lan-Ting Liu(刘兰亭)[1,2]

[1] *Fundamental Science on Aircraft Structural Mechanics and Strength Laboratory, Northwestern Polytechnical University, Xi'an* 710072, *China*
[2] *School of Aeronautics, Northwestern Polytechnical University, Xi'an* 710072, *China*
[3] *College of Materials Science and Engineering, Xi'an Shiyou University, Xi'an* 710065, *China*

(Received 8 May 2020; revised manuscript received 13 June 2020; accepted manuscript online 6 July 2020)

Tensile behaviors of Ti/Ni nanolaminate with model-I crack are investigated by molecular dynamics simulations. The Ti/Ni nanolaminates with center crack either in Ti layer or in Ni layer under different loading directions are utilized to systematically study the mechanical performance of the cracked material. The results indicate that pre-existing crack dramatically changes the plastic deformation mechanism of the Ti/Ni nanolaminate. Unlike the initial plastic deformation originating from the interface or weak Ti layer of the crack-free samples, the plastic behavior of cracked Ti/Ni nanolaminate first occurs at the crack tip due to the local stress concentration. Subsequent plastic deformation is dominated by the interaction between the crack and interface. The Ti/Ni interface not only impedes the movement of the initial plastic deformation carriers (dislocation, slip band, and deformation twinning) from the crack tip, but also promotes the movement of interfacial dislocations in the tension process. Microstructure evolution analysis further confirms that the plastic deformation mechanism transition is ascribed to the orientation-dependent tensile behavior at the crack tip, which is intrinsically attributed to the anisotropy of the certain crystal structure and loading direction of the cracked Ti/Ni nanolaminate. In addition, by analyzing the effects of different plastic deformation carriers on crack propagation in specific crystal, it can be discovered that the interfacial dislocations moving towards the crack tip can further promote the crack growth.

Keywords: molecular dynamics, Ti/Ni nanolaminate, plastic deformation mechanisms, crack propagation

PACS: 62.25.–g, 68.65.Ac, 62.20.F–, 62.20.mt **DOI:** 10.1088/1674-1056/aba2e5

1. Introduction

Ti/Ni nano-laminated material fabricated by alternately depositing hexagonal close-packed (HCP) and face-centered cubic (FCC) metal is widely used in high-tech fields due to its marvelous optical,[1,2] magnetic,[3] and reactive properties.[4,5] And these unique properties are closely related to the HCP/FCC heterointerface in the Ti/Ni nanolaminate. Besides considerable investigations of above physical and chemical properties, quite a few researchers focus on exploring the mechanical properties of Ti/Ni nano-laminated materials. And the novel mechanical properties, such as orientation-dependent hardness and size-dependent strain rate sensitivity transition, could be obtained in as-deposited and annealed Ti/Ni nanolaminate.[6–9] However, the role of dense interface in the mechanical properties of Ti/Ni nanolaminate is still unclear. To ensure the high-efficiency use of the material, more attention should be paid to the effect of the interface on the mechanical behavior of Ti/Ni nanolaminate.

There are dense interfaces in the internal metallic nanomaterials, therefore the effects of different interfaces on the mechanical performance of nanomaterials should be meticulously taken into consideration. Fruitful investigations have shown that internal interfaces significantly influence mechanical behaviors of the metallic nanomaterials.[10–12] Nano-laminated materials are a kind of two-dimensional metallic nanomaterial, where dense interfaces (crystalline/crystalline, crystalline/amorphous, and amorphous/amorphous interfaces) are formed at the junction of the components. Therefore, the interfaces also dramatically affect the mechanical performance of the nano-laminated material.[13,14] Numerous experiments and molecular dynamics (MD) simulations indicate that the interface structure is a key factor that determines the mechanical properties of the nanolaminate. The interfaces can serve as sources, sinks and barriers for incoming plastic deformation carriers (dislocations, twinning, slip bands, and shear bands), resulting in the dramatic enhancement in strength and ductility.[15–19] For the most studied crystalline/crystalline interfaces, the interfaces can be further divided into transparent and opaque interfaces according to their matching degrees of adjacent lattices.[16] Transparent interface is often formed between two layers with the same crystal structure, such as Cu/Ni (FCC/FCC) and Cu/Ag (FCC/FCC) interfaces. Transparent interface has little resistance to dislocations movement

*Project supported by the National Natural Science Foundation of China (Grant No. 11572259), the Program for International Cooperation and Exchanges of Shaanxi Province, China (Grant No. 2016KW-049), the Natural Science Foundation of Shaanxi Province, China (Grant No. 2019JQ-827), and the Scientific Research Program Funded by Shaanxi Provincial Education Department, China (Grant No. 19JK0672).

†Corresponding author. E-mail: dengqiong24@nwpu.edu.cn
‡Corresponding author. E-mail: amr_lr@126.com

© 2020 Chinese Physical Society and IOP Publishing Ltd

due to the same slip systems of the two adjacent layers. And the resistance against dislocations passing through the interface mainly comes from the coherent strain.[16,20] Opaque interface is often formed between two layers with different crystal structures, and most widely studied interface is about the Cu/Nb (face-centered cubic/body-centered cubic, FCC/BCC) interface. Slip systems on both sides of an opaque interface are usually discontinuous, and the interface becomes a barrier to dislocations slip.[11] The interaction between opaque interface and dislocation is more complicated than that of a transparent interface. The dislocation propagation will be impeded by the interface, which leads to the high strength of the material. At the same time, the interaction between the interface and dislocation provides effective plastic deformation path to promote better plasticity.[21–23] However, most of the current studies focus on the FCC/FCC and FCC/BCC interfaces, while the study of HCP/FCC interface has been rarely reported except that by An *et al*.[24] They performed MD simulations to evaluate the effects of coherent (transparent) and incoherent (opaque) interfaces on the tensile behaviors of Ti/Al (HCP/FCC) nanolaminates. The results demonstrated that plastic deformation mechanism varies with the interfacial structure. And the interface-dependent plastic deformation is due to different mismatch dislocation networks forming at the interface and different slip systems of gliding dislocations in Ti and Al layers. Although HCP/FCC nanolaminate is a kind of functional material, the role of the interface on the mechanical performance and interaction between HCP/FCC interface and different defects are still unclear.

The microcrack can be unavoidably generated in the brittle interlayers or interface between the nano-laminated composites in the preparation process. These microcracks strikingly reduce the strength of the materials by introducing local stress concentration. Furthermore, the crack propagation and interaction with interface will greatly affect the toughness of the material.[25–27] In contrast to fruitful work focusing on strength of the nanolaminates, only a small amount of work has been done to explore the toughness of the nano-laminated materials. Zhang *et al*. performed uniaxial tensile testing to study the fracture behaviors of various FCC/BCC nanolaminates, and they found that the microcracks are initiated from the brittle layer but blocked by the interface, resulting in the improvement in the toughness of the Cu/X nanolaminates.[25] Li *et al*. used MD method to study the crack propagation behavior in Cu/Nb nanolaminates, and found the weak Cu/Nb interface can suppress the crack propagation in two ways: interfacial dislocation nucleation relieves the high stress at the crack tip; interface can also blunt the crack tip through interfacial slip.[27] The current work has revealed that the interface can impede the crack propagation. However, the specific mechanism of the interplay between crack and different interphase interfaces, especially HCP/FCC interface, is still unclear. Therefore, a lot of investigations are needed to obtain the interaction mechanism of crack and interface in different types of nano-laminated materials.

In this work, the MD method is performed to reveal the effect of crack on the tensile behavior of Ti/Ni nanolaminate. The center crack is introduced to explore the interaction between the interface and crack. The results indicate that pre-existing crack significantly changes the strength and plastic deformation mechanism of the Ti/Ni nanolaminate. The propagation of the interfacial dislocations and their interaction with plastic deformation carries initiated from crack dominate the plastic deformation of the material. All these results have great significance for promoting the theoretical research and practical application of Ti/Ni nano-laminated materials.

2. Simulation methods

To investigate the role of crack and interface in the tensile behavior of Ti/Ni nano-laminated composites, the various mode-I crack models are established. Considering the components (crystallographic structures and orientations) also have great impact on the overall mechanical properties of the nanolaminates, four cracked models with crack in different layers (Ti or Ni layer) under different loading directions (parallel or perpendicular to the interface) are employed to systematically study the tensile behaviors of cracked Ti/Ni nanolaminates. The schematic of cracked Ti/Ni nanolaminates under different loading directions is depicted in Fig. 1, and initial crystalline orientations of Ti and Ni are also plotted at the bottom of Fig. 1. In the present study, the thickness of the top layer and the thickness of the bottom layer are both set to be 6.10 nm, while the thickness of the middle layer is assumed to be 12.16 nm. Hence, modulation ratio R is fixed at 1:1 in all specimens. The total length in the Z direction is 24.36 nm, and the size in the X direction and the size in the Y direction are 3.54 nm and 18.99 nm, respectively. The microcrack is established by removing a portion of the atoms in the center of the structure. The length of the microcrack is 2.93 nm, which is three times larger than the cut-off radius. Periodic boundary conditions (PBCs) are used in all directions to eliminate surface effect and pay more attention to the role of crack and interface in the mechanical properties of the cracked Ti/Ni nanolaminates. For comparation, the same-sized crack-free Ti/Ni nanolaminates under different loading directions are also built. It is known that different stacking orders and surfaces may result in different mechanical properties of crack-free nano-laminated material in nanoindentation testing.[19] However, the PBCs are applied in all directions to form an infinite crack-free Ti/Ni sample. Thus, different stacking orders have negligible effect on the tensile behaviors of crack-free sample in this work. For convenience, the crack-free model

with a middle Ti layer is discussed only in the present work as shown in Fig. 1. The most closed-packed planes of Ti (0001) and Ni (111) are stacked along the Z direction in all models, as the gaseous atoms prefer to deposit along those planes to gain the minimum energetic state during the preparation.[6–9]

The interatomic potential is vital for the accuracy of the MD simulations, the embedded atomic method (EAM) potential[28,29] is utilized to predict atomic interaction for various atoms, which has been successfully used to describe the mechanical behaviors of nano-laminated materials of Ti/Al,[24] Cu/Au,[30] Cu/Ni,[31] and Cu/Ag.[32] During the simulation, Verlet integral algorithm is used to describe the motion of the newton atoms, and the time step is fixed at 3 fs (10^{-15} s). To reduce the thermal vibration of the system, the near-zero temperature of 0.01 K is selected to catch the effect of true strain energy on the plasticity of the crack and interface. Before being loaded, samples are first relaxed at NVT ensemble to reach a minimum energetic state. After that, tension loading is implemented by uniformly giving a constant strain of 0.0005 to all the atoms. Then, the system is relaxed to a new equilibrium state. These tension-relaxation processes are repeated until the tensile strain arrives at 0.25. Atomic stress of the model is obtained through the Virial theorem.[33] To observe the atomic configuration evolution, open visualization tool (OVITO)[34] is employed, where numerous powerful modules are integrated in the software. The atomic configurations and the defects in nanocrystal are visualized through common neighbor analysis (CNA),[35] the FCC, BCC, HCP, and non-structure atoms are marked in green, blue, red, and light gray, respectively. The dislocation motion in the tension process is identified by the dislocation extraction algorithm (DXA).[36]

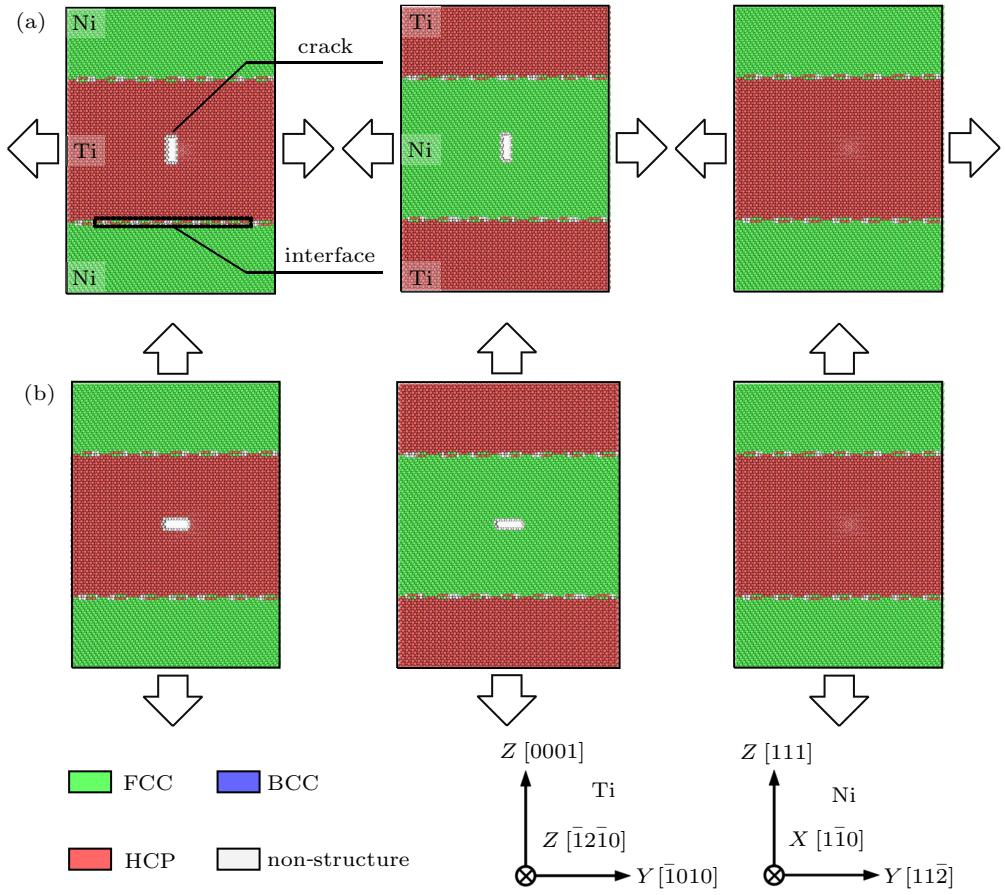


Fig. 1. Schematic diagram of cracked and crack-free Ti/Ni nanolaminates with tension loading applied along (a) Y direction and (b) Z direction. Atoms are colored according to the CNA method. And coordinate systems represent the initial crystalline orientation of Ti and Ni, respectively.

3. Results and discussion

3.1. Tensile properties of cracked Ti/Ni nanolaminates

Figure 2 shows the stress–strain curves of disparate Ti/Ni nanolaminates with tension loading applied along different directions. Linear stages of the stress–strain curves for different models almost overlap, implying that the microcrack has little influence on the elastic properties of the Ti/Ni nanolaminates. However, yield stress (the endpoint of the linear elastic stage) of the cracked model is lower than that the crack-free Ti/Ni nanolaminate has, indicating the pre-existing crack truly reduces the strength of the Ti/Ni nanolaminate. After reaching the peak stress (maximum value in the stress–strain curve), the stress of the crack-free sample drops rapidly, while the stress of cracked sample maintains a relatively high value

in the tension processes. It demonstrates that plasticity of cracked Ti/Ni nanolaminate is better than that of the crack-free Ti/Ni nanolaminate, which is ascribed to the couple effect of the Ti/Ni interface and crack. The stress–strain relationship provides the overall tensile response of Ti/Ni nanolaminate in a certain loading direction, and microstructure evolutions of different Ti/Ni nanolaminates are displayed in the following parts.

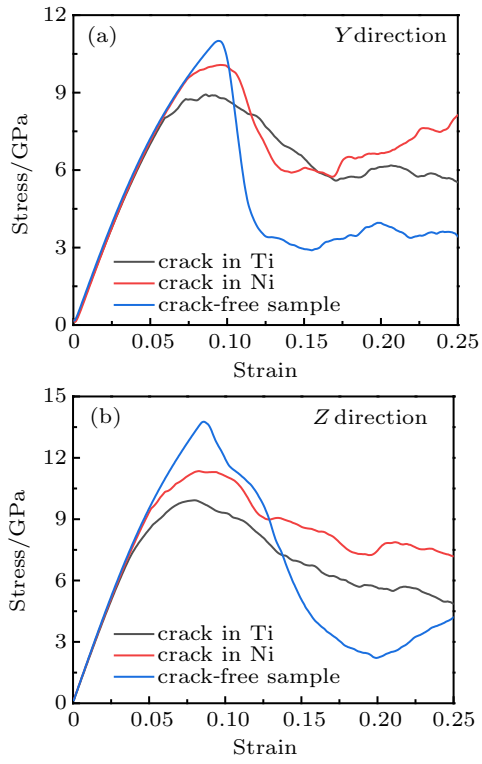


Fig. 2. Stress–strain curves of disparate Ti/Ni nanolaminates in different loading directions: (a) Y direction and (b) Z direction.

3.2. Tensile behaviors of cracked Ti/Ni nanolaminates with loading applied parallelly to interface

To reveal the role of the interface in the tensile behavior of Ti/Ni nanolaminate, the relaxation properties of Ti/Ni interface in crack-free sample are first shown in Figs. 3(a) and 3(b). Different crystal structures of atoms are colored according to the CNA method. In this work, semi-coherent Ti (0001)/Ni (111) interfaces with the periodic mismatch dislocation networks are formed at the junction of two crystals, corresponding stress distribution in the Y direction is also shown in Figs. 3(a′) and 3(b′). In the atomic stress distribution diagram, the atoms are colored according to the value of the Virial stress in the tensile processes. Although misfit dislocations balance the local strain, the stress distribution of the interface changes profoundly. There is stress concentration at the nodes (dash circles), which are the intersection of dislocation networks. The nodes of interface in Ti layer bear larger positive stress, while nodes of interface in Ni layer bear larger negative stress. Positive stress indicates that the atoms are in the tensile state, and vice versa. Generally, the reason for the complex stress distribution at the interface is the mismatching of lattice parameters in different components. Due to the complex microstructure and stress distribution of the interface, dislocations and other plastic deformation carriers will probably nucleate and evolve from the interface. The interface can serve as a source and sink of these plastic deformation carriers, which promotes the ability to sustain the deformation of the material.[22–24]

Figures 3(c)–3(f) show the microstructure evolutions of the crack-free Ti/Ni nanolaminate. The sample first yields at a strain of 0.098, which is defined as the yield point. Some BCC embryos are generated in Ti layer neighboring the interface, and dislocations nucleate in Ni layer near the interface. The growth of BCC embryos and dislocations facilitates stress releasing at the interface as shown in Fig. 3(c′). Upon being further loaded, the BCC-Ti grows fleetly to reach the opposite interface, partial dislocations with $b_1 = 1/6\langle 112\rangle$, shown by black circles in Fig. 3(d), evolve from interface and slide along the $\{111\}$ planes in Ni layer. At a tensile strain of 0.109, the FCC–Ti nucleates and grows quickly in Ti layer, and vast partial dislocations glide in Ni layer until they are absorbed by the opposite interface. Finally, the entire HCP phase transforms into the FCC phase in Ti layer, with a certain number of HCP stacking faults left at the internal Ti layer. Dislocation propagation dominates the subsequent plastic behavior of Ni layer. As shown in Fig. 3, allotropic phase transformation is observed in Ti layer in the tension process. Generally, phase transformation is observed during mechanical testing of HCP material due to a finite slip system. The HCP material can achieve plastic deformation through phase transformation under a certain crystal structure and loading mode.[37–40] Atomic shuffle of the basal atoms contributes to the transient phase transformation of HCP-to-BCC structure.[39,40] In this work, due to stress concentration at the Ti/Ni interface, atoms around the interface are more easily to active the atomic shuffle, thus the BCC atoms first emerge near the interface. While the phase transformation of BCC-to-FCC structures is mainly caused by dense dislocation propagation and accumulation of FCC stacking faults.[39,40] For the tensile behavior of crack-free Ti/Ni nanolaminate with loading applied parallel to the interface, the allotropic phase transformation of HCP–BCC–FCC dominates the plastic deformation in Ti layer, and continuous dislocation propagation dominates the plastic behavior in Ni layer. Interface in crack-free Ti/Ni nanolaminate can not only act as dislocations source and sink, but also promote the phase transformation in Ti layer.

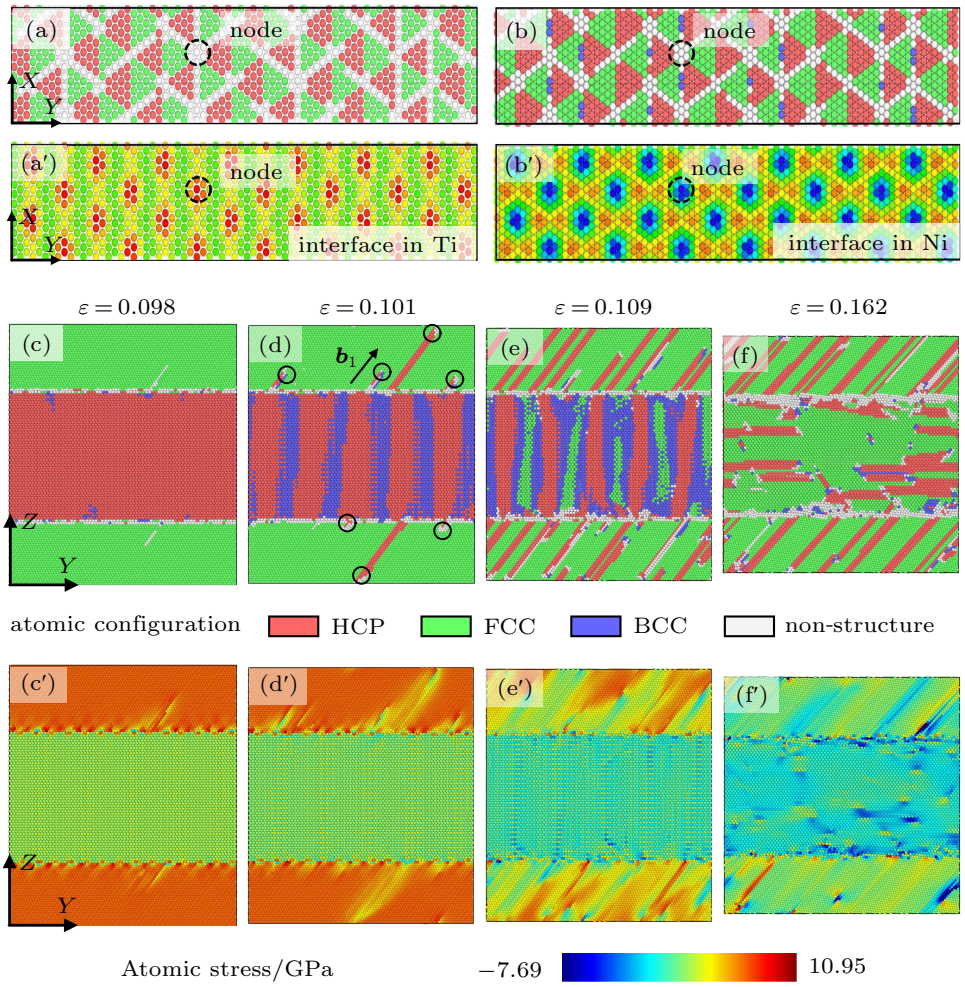


Fig. 3. Microstructure evolutions and atomic stress evolutions of crack-free Ti/Ni nanolaminate with tension loading applied along the *Y* direction, showing [(a) and (b)] relaxation configuration of Ti/Ni interface, (c)–(f) microstructure evolutions at various tensile strains, where atoms are colored according to the CNA method, (a′)–(f′) corresponding atomic stress evolutions, where atoms are colored according to the value of the Virial stress.

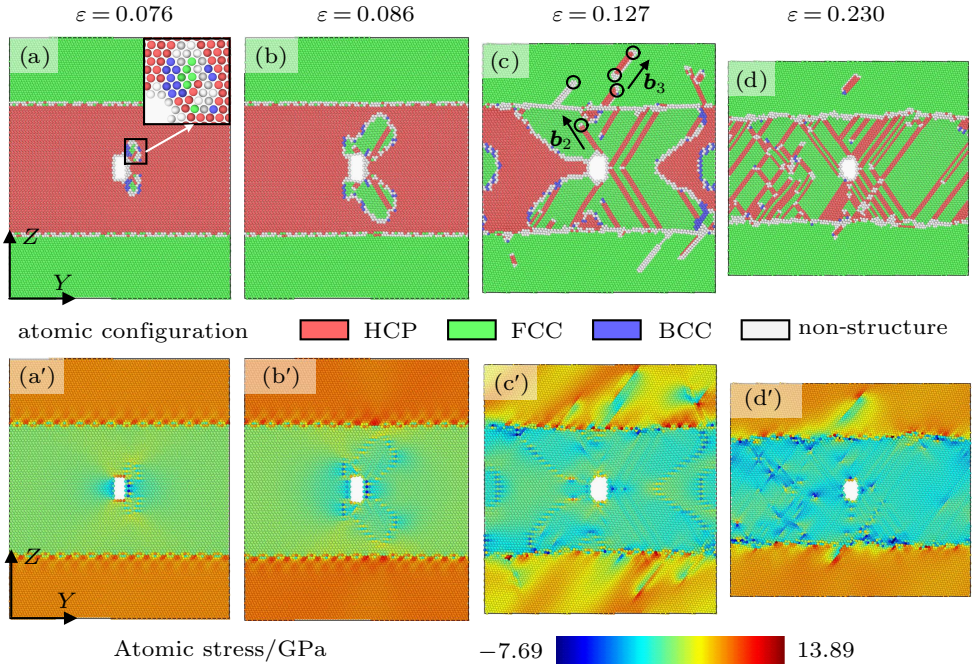


Fig. 4. Microstructure evolutions and atomic stress evolutions of Ti/Ni nanolaminate with crack in Ti layer under tension loading applied along *Y* direction, showing [(a)–(d)] microstructure evolutions at various tensile strains, atoms are colored according to CNA method, (a′)–(d′) corresponding atomic stress evolutions, atoms are colored according to Virial stress value.

The plastic deformation behaviors of the Ti/Ni nanolaminate with crack in Ti layer are shown in Fig. 4. Unlike the crack-free Ti/Ni nanolaminate, the plastic deformation first occurs at the crack tip. At a strain of 0.076, FCC–Ti nucleates at the blunt crack tip. Corresponding stress distribution diagram demonstrates that the stress concentration on the crack tip facilitates the formation of new phase. Upon being further loaded, the FCC phase grows quickly until the grain boundaries reach the interface. And the stress distribution shows that high stress near the crack front is released by expanding new grains as shown in Fig. 4(b). The phase transformation of HCP-to-FCC structure in Ti layer is also related to the dislocation propagation and accumulation of dense stacking faults.[37–40] Go on loading, the FCC grains gradually grow in Ti layer, and some partial dislocations with $\boldsymbol{b}_2 = 1/6\langle 112\rangle$ nucleate and arise from the crack tip in FCC regions. A mass of partial dislocations with $\boldsymbol{b}_3 = 1/6\langle 112\rangle$ initiated from the interface and are absorbed by the opposite interface in Ni layer as shown by black circles in Fig. 4(c). At larger tensile strain, the interaction between interfacial dislocations and dislocations initiated from the interface dominates the plastic behaviors in FCC–Ti layer.

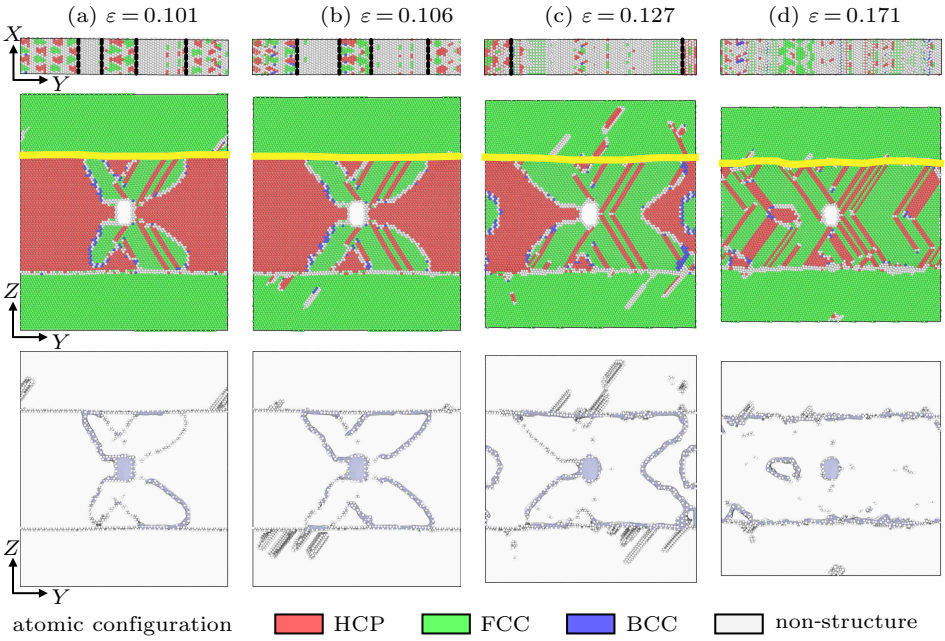


Fig. 5. Interactions between crack and Ti/Ni interface at strain (a) 0.101, (b) 0.106, (c) 0.127, and (d) 0.171. Top panels are atomic configurations of Ti/Ni interface in Ni layer, middle panels are microstructure evolutions of cracked nanolaminate, and bottom pictures are corresponding defect propagations at various tensile strains. Atoms are colored according to CNA method.

Figure 5 shows the details of the interaction between the crack and Ti/Ni interface, and the microstructure evolutions after FCC grain boundaries have reached interface. The middle panels in Fig. 5 displays the atomic configuration evolutions at various strains, while the top and bottom panels show the microstructure of interface in Ni layer and defect propagations at corresponding tensile strains. At the tensile strain of 0.101, the FCC grain boundaries reach the interface, leading to the original mismatch dislocation networks to break down, partial semi-coherent interface turns into an incoherent region as shown by the dash line on the top of Fig. 5(a). Simultaneously, dislocations nucleate at the Ti/Ni interface and propagate in Ni layer. With the loading going on, the FCC grains grow parallel to the interface in Ti layer, resulting in the expansion of the incoherent interface. While partial dislocations nucleate and glide in FCC–Ti layer and Ni layer as described in Figs. 5(b) and 5(c). At a strain of 0.171, the incipient HCP phase has completely transformed to the FCC phase, where dense HCP stacking faults form in the Ti layer due to nucleation and propagation of numerous dislocations from the crack tip. At this moment, the Ti/Ni interface integrally becomes incoherent interface. The yellow lines in the middle picture indicate that none of incoherent interfaces is of planar structure. Continuous dislocation emission and absorption ultimately lead to the rugged interface. Moreover, interfacial dislocations propagate and interact with the dislocations or stacking faults, which consumes the energy of the system and leads to the stable plastic flow stress. In the tensile process, the semi-coherent Ti/Ni interface is a barrier to defect expansion and provides nucleation sites for various plastic deformation carriers. While for the succeeding incoherent interface, the interface can serve as the dislocation source to maintain the steady plastic deformation in the adjacent layer. Although the microcrack reduces the strength of the nanolaminate, the interaction between dislocations evolving from the crack tip and the interfacial dislocations guarantees the better plastic properties of the cracked nanolaminate.

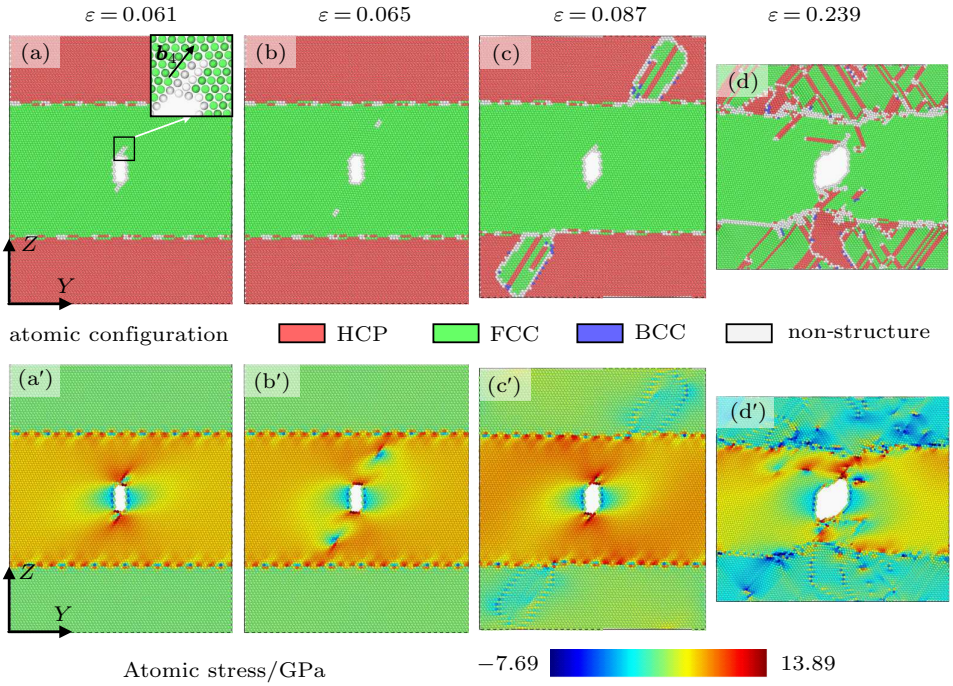


Fig. 6. Microstructure evolutions and atomic stress evolutions of Ti/Ni nanolaminate with crack in Ni layer under tension loading applied along Y direction, showing [(a)–(d)] microstructure evolutions at various tensile strains, where atoms are colored according to CNA method, [(a′)–(d′)] corresponding atomic stress evolutions, where atoms are colored according to Virial stress value.

As for the case of crack in Ni layer, the first full dislocation with $\boldsymbol{b}_4 = 1/2\langle 110\rangle$ nucleates and emits from the crack tip to release the high stress around the crack front. With tension process going on, the full dislocations glide along the $\{111\}$ planes until they are absorbed by the Ti/Ni interface as shown in Fig. 6(b). The absorption of dislocations leads the semi-coherent interface and stress concentration to gradually destruct in the opaque interface. Thus, the stress-induced phase transformation of HCP to FCC structure is easier to trigger in a Ti layer as shown in Fig. 6(c). With the increase of tensile strain, full dislocations and multiple dislocations continuously emitting from the crack tip lead the cracks to propagate in Ni layer. At the same time, HCP–Ti is finally completely converted into the FCC phase, leaving a large number of HCP stacking faults in Ti layer. It is worth pointing out that the plastic behavior first occurs at the crack tip for the cracked sample. This phenomenon is different from the initial plastic behavior of cracked Cu/Nb nanolaminate, in which the partial dislocations first nucleate at the weak Cu/Nb interface.[27] In this work, the semi-coherent Ti/Ni interface is a strong interface, the critical stress to initiate plasticity in Ti/Ni interface is larger than that of the crack tip. Furthermore, the yield stress and strain of the perfect model are 11.002 GPa and 0.098, which are higher than the yield stress and strain of cracked model, indicating that the Ti/Ni interface can withstand greater elastic deformation and higher elastic stress. Therefore, initial plasticity turns to occur in another stress-concentrated area, i.e., crack tip, as the lower stress is required to evolve plastic behavior in cracked Ti/Ni nanolaminate.

As shown in Figs. 3–6, pre-existing microcrack leads to great changes in the plastic deformation mechanism of Ti/Ni nanolaminate with loading applied parallel to the interface. The local stress state may greatly change the deformation mode of the material. For the crack-free sample, the plasticity first occurs nearby the Ti/Ni interface due to the local stress concentration on the interface, the phase transformation of HCP to BCC structure in Ti layer and dislocations gliding in Ni layer dominate the initial plastic behavior of Ti/Ni nanolaminate. As for the sample with crack in Ti layer, the initial plastic behavior first occurs at the crack tip, and the phase transformation of HCP to FCC structure arises due to the stress concentration at the crack tip. While for the sample with a crack in Ni layer, primary plastic behavior is full dislocations gliding along a certain plane near the crack tip with the stress concentrating on the crack tip. Moreover, subsequent plastic behaviors of cracked samples contain the propagation of plastic deformation carries and their interaction with the interface. Therefore, microcrack significantly reforms the stress distribution of the Ti/Ni nanolaminate, leading the plastic behaviors to occur first at the crack tip. The interaction between the defects initiated from the crack tip and interfacial defects improves the plastic properties of the material, and eventually causes the vital difference in the plastic deformation mechanism between the crack-free and cracked Ti/Ni nanolaminate.

3.3. Tensile behaviors of cracked Ti/Ni nanolaminates with loading applied perpendicularly to the interface

As described above, microcrack has great influence on the plastic deformation of Ti/Ni nanolaminate with tension loading applied parallel to the interface. Further exploring of

the deformation behaviors of Ti/Ni nanolaminate with loading applied perpendicular to the interface, the atomic configuration evolutions of different models are shown in Fig. 7. The deformation behaviors are markedly different from the case of tension loading applied parallel to the interface, showing the orientation-dependent behavior in the tension process. Figure 7(a) shows the plastic behaviors of Ti/Ni nanolaminate with crack in Ti layer. The slip band (indicated by the yellow arrow) first emits from the crack tip at a tensile strain of 0.039, which glides along the $(10\bar{1}1)$ pyramidal plane before reaching the Ti/Ni interface as shown in Fig. 7(a). The pyramidal slip band was also discovered in tensile process of cracked Mg and Ti materials, in which the crystallographic orientation of the initial crack was also $(0001)[10\bar{1}0]$.[41,42] Therefore, pyramidal slip band is also in an important plastic deformation form at the crack tip in HCP-based material. As the stretch process continues, the slip bands arrive at the interface and are absorbed by the interface, leading the stress distribution to vary at the interface. The new grains nucleate and grow near the interface at the internal Ti layer. Concurrently, dislocations nucleate from the interface and propagate in the Ni layer. At a strain of 0.076, two twin variants with different crystalline orientations are discovered in the internal Ti layer. To better clarify the orientation relationship between the matrix and twin variants, the deformed sample is sliced perpendicular to the $[1\bar{2}10]$ axis of the matrix as shown in the inset of Fig. 7(b). Meanwhile, the local crystalline axes are also plotted in the respective grains. As shown in the illustration, the basal planes ($\{0001\}$ planes) of matrix and variant I are perpendicular to the observational plane, and the basal plane of variant II is located in the observed plane. It should be noted here that

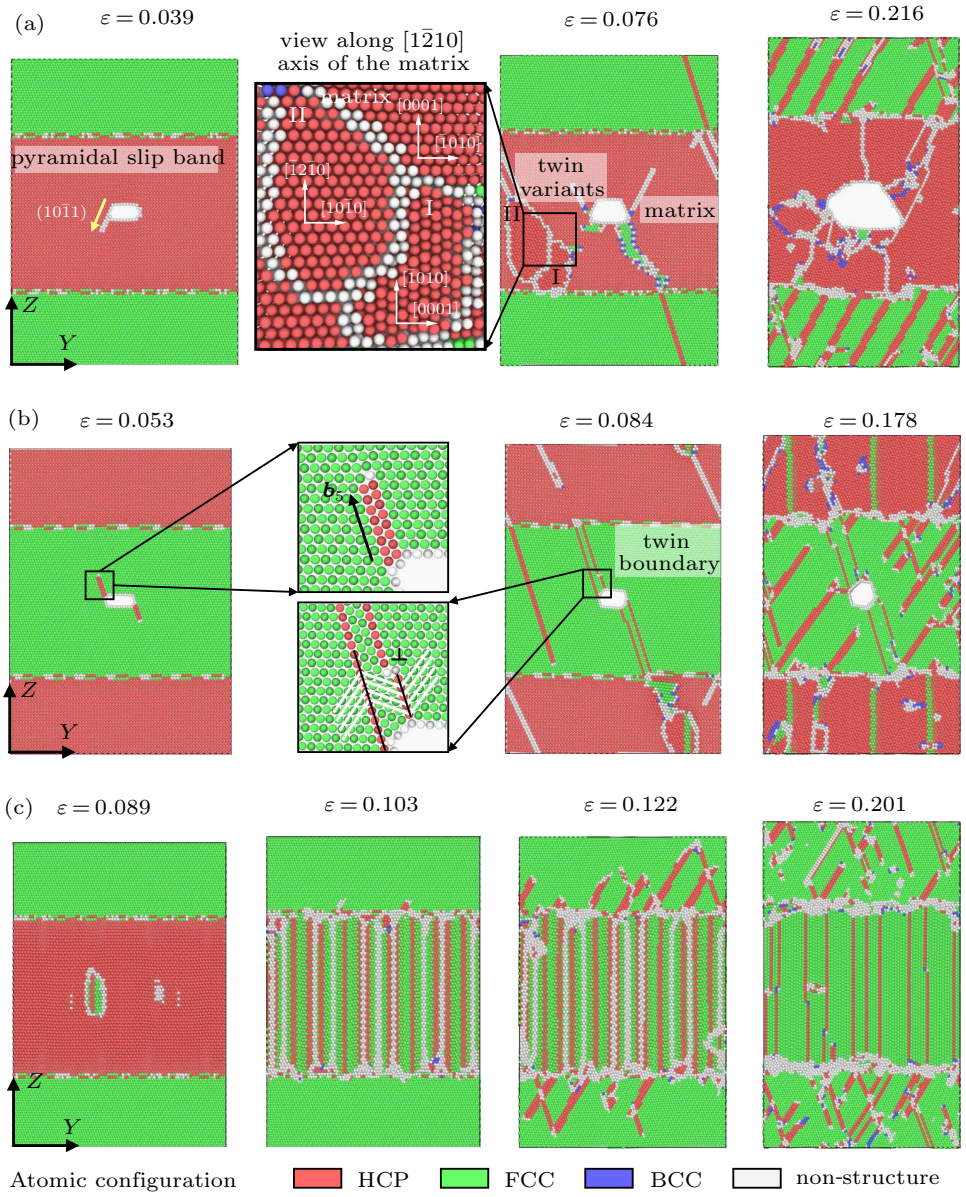


Fig. 7. Microstructure evolutions of Ti/Ni nanolaminates with tension loading perpendicular to the interface, showing (a) Ti/Ni nanolaminate with crack in Ti layer, (b) Ti/Ni nanolaminate with crack in Ni layer, (c) crack-free Ti/Ni nanolaminate, where atoms are colored according to CNA method. Insets display enlarged details in the tensile process.

the basal planes of the two twin variants are perpendicular to the basal plane of the matrix. And the angle between the basal planes of the matrix and variants is slightly larger than the angle of $\{10\bar{1}2\}\langle 10\bar{1}1\rangle$ twins, in which the crystal orientations on the two sides differ by 84.78°, theoretically. Therefore, the grain reorientation in the present work is a twinning-like behavior. The concrete mechanism and the orientation relationship between matrix and twins have been discussed in our previous work of perfect Ti/Ni nanowires,[43] indicating that the grain reorientation behavior is favored with loading applied in the Z direction. At the large strain, the grain reorientation is completed in Ti layer, the twinning continually generates from the crack tip. Meanwhile, numerous dislocations are activated and finally absorbed by opposite interface in Ni layer. Twinning in crack tip and dislocation propagation in Ni layer ensure the good plasticity of cracked nanolaminate. As for the crack in Ni layer, partial dislocations with $\boldsymbol{b}_5 = 1/6\langle 112\rangle$ sprout first from the crack tip to release high stress. Thereafter, partial dislocations continually emit from the crack tip and glide along the adjacent planes, resulting in the abnormal deformation twinning in Ni layer (enlarged illustration of Fig. 7(b)), which is consistent with the results in cracked Al and Ni.[44–46] Upon being further loaded, dislocations nucleate from the interface, glide in Ni layer, and interact with twin boundaries, and grain reorientation also takes place in Ti layer, which maintains good plasticity of cracked nanolaminate. Deformation behavior of crack-free Ti/Ni nanolaminate is presented in Fig. 7(c). The FCC embryos first emerge in the weakened Ti layer and gradually grow until they reach the interface, leading the interfacial structure to be destructed. Then a series of partial dislocations nucleates from the interface and interacts with each other in Ni layer. Like the tensile behaviors of the sample with loading applied along the Y direction, the pre-existing crack induces the plasticity to initially occur at the crack tip, resulting in the plastic deformation mechanism transitioning between the crack-free and cracked Ti/Ni nanolaminates. The interaction between the plastic deformation carriers generating from the crack tip and the interface makes the cracked Ti/Ni nanolaminates possess more abundant plastic deformation capacity, thus showing better plastic properties than crack-free models. Namely, the microcrack indeed changes the stress state inside the nano-laminated material, resulting in a significant variation in the plastic deformation mechanism of Ti/Ni nanolaminates.

3.4. Orientation-dependent tensile behaviors at crack tip

As mentioned above, different initial plastic behaviors at the crack tip finally lead the plastic deformation mechanism to transition for the cracked Ti/Ni nanolaminate. Thus, orientation-dependent tensile behavior at the crack tip should be concerned to seize the nature of different plastic deformation mechanisms.

Figure 8 summarizes plastic behaviors at the crack tip for different cracked Ti/Ni nanolaminates. In a panel, number 1 or 2 refers to microstructure evolution at the crack tip, which is visualized by the CNA method, while number 3 or 4 means its corresponding dislocation or other defect distribution, which contains crack, grain boundary, slip band and twin boundary, shown by the gray mesh in the graphs. The dislocation lines are colored according to the DXA method in specific crystal, and the gray arrow denotes the Burges vector of respective dislocation. For the better observation, atoms in defect distribution diagram have been removed. It can be seen from Fig. 8 that defects are initiated from the crack tip and propagate in a ductile manner, which evolves through dislocation propagation or deformation twinning rather than brittle cleavage. As tension loading is parallel to the interface, the phase transformation of HCP to FCC structure in the Ti layer occurs first at the crack tip as shown by the black rectangle in panel 1 of Fig. 8(a). Due to the difference in crystal lattice, there are dislocations existing at junction of two phases as shown in panel 3 of Fig. 8(a). Then, partial dislocations with Burges vector of $\boldsymbol{b}_2 = 1/6\langle 112\rangle$ arise from the crack tip and interact with the interfacial dislocations in FCC Ti. While for the model of crack in Ni layer, full dislocations (blue lines, which are perpendicular to the observational plane) with Burges vector of $\boldsymbol{b}_4 = 1/2\langle 110\rangle$ first emit from the crack tip. And subsequent multiple dislocations, which contain partial dislocations and stair-rod dislocations, sprout from patulous crack tip and interact with the dislocations generating from the interfaces as shown in Fig. 8(b). For the case where the tension loading is perpendicular to the interface, slip band emits first from the crack tip and glides along the $(10\bar{1}1)$ plane in Ti layer. The DXA indicates that the dislocation motions cannot be activated under this loading condition, and the pyramidal slip band turns to be emitted at the crack tip, as plotted in panels 1 and 3 of Fig. 8(c). After the completion of grain reorientation, the deformation twinning turns to be generated from the crack tip, and the analysis of DXA demonstrates that there are little dislocation motions near the crack tip under this loading condition as shown in panels 2 and 4 of Fig. 8(c). For the last case, the partial dislocation with Burges vector of $\boldsymbol{b}_5 = 1/6\langle 112\rangle$ is continually emitted from the crack tip and glides along the adjacent plane, resulting in the deformation twinning at the crack front as shown in Fig. 8(d).

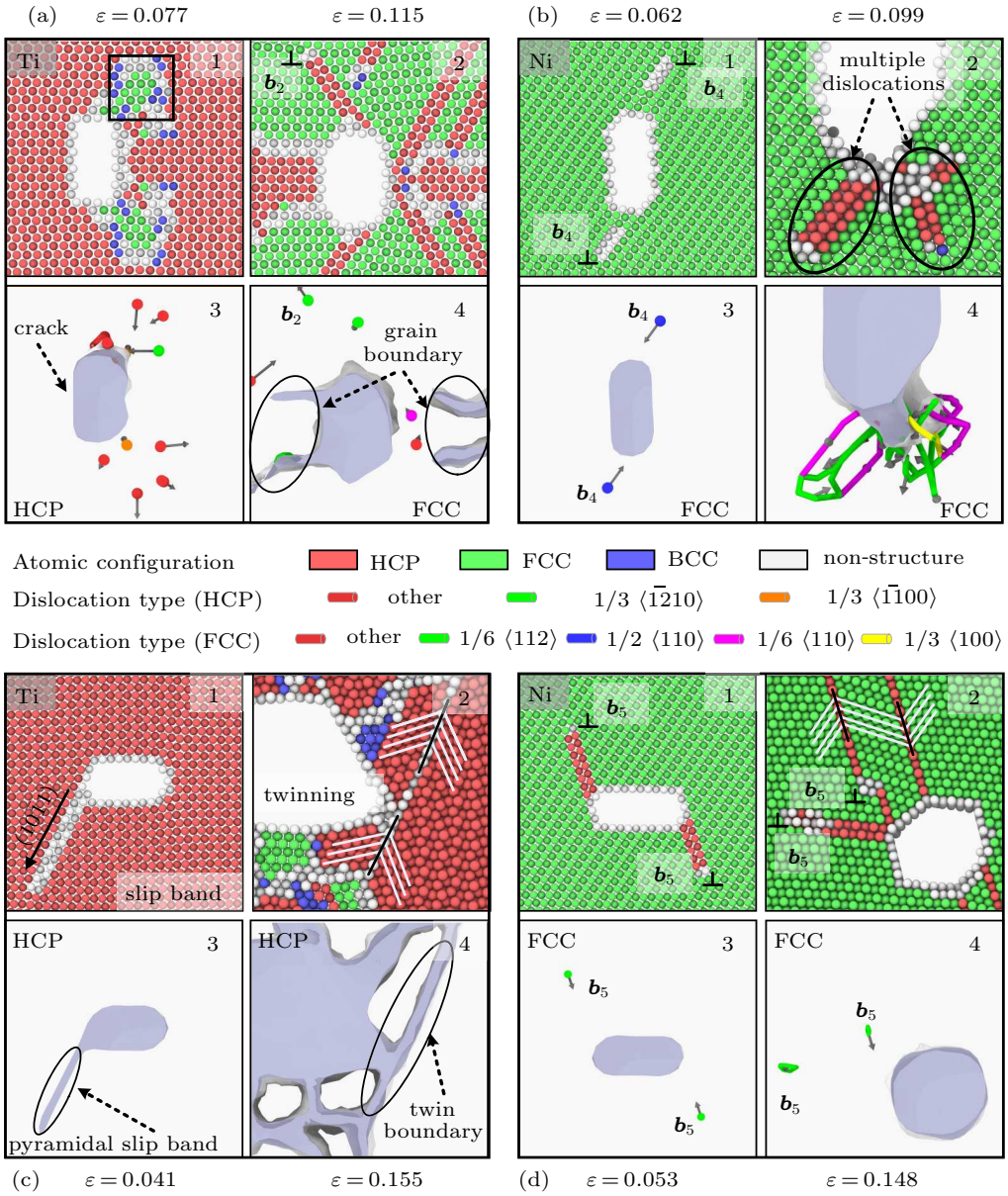


Fig. 8. Crack propagations in different loading directions for Ti/Ni nanolaminates, with crack in (a) Ti layer and (b) Ni layer with loading applied along *Y* direction, and crack in (c) Ti layer and (d) Ni layer with loading applied along *Z* direction. In panel, number 1 or 2 shows the atomic configuration, which is colored according to the CNA method, 3 or 4 displays corresponding defect distribution, which is identified by the DXA method. In panel, 1 or 2 shows the atomic configuration, which is colored according to the CNA method, 3 or 4 displays the corresponding defect distribution, which is identified by the DXA method.

Table 1 summarizes the main plastic behaviors of crack tips in different tension loading directions. For comparison, the models with crack in pure Ti and pure Ni are also listed. Orientation-dependent tensile behavior at the crack tip is presented in Table 1. Essentially, anisotropic plasticity is related to crystallographic orientation of Ti and Ni in the specific tension process. As the loading applied along the *Y* direction, Ti $[\bar{1}010]$ crystalline axis bears the tension loading. The phase transformation and subsequent dislocation propagation in HCP Ti are favored in this direction.[37–39] For the loading applied along the *Z* direction, the tension loading is applied along the Ti [0001] crystalline axis. The grain reorientation and deformation twinning in Ti layer are supported under this loading condition.[38] Additionally, the full dislocations or deformation twinning in cracked Ni layer are formed due to the movement of partial dislocations in different slip planes.[45] The first partial dislocation is emitted from the crack tip, leaving the stacking faults in the front of crack . And the second partial dislocation is crucial for subsequent plastic behavior. If the trailing partial dislocation propagates along the same plane as the leading dislocation and Burges vector of trailing partial dislocation is complementary to the leading dislocation, then the stacking faults are erased by the trailing dislocation and full dislocations are formed. If the trailing partial dislocation propagates along the adjacent plane with the same Burges vector as the leading dislocation, then the twining partial dislocation erases stable stacking faults and forms the twin faults at the crack tip. This “microtwin” grows with the applied stress increasing and finally forms the twinning at the crack tip.[45]

Table 1. Main plastic behavior around crack tip in different loading directions.

Orientation	Models	Crack	Plastic behavior	Burgers vector
Y direction (parallel to the interface)	Ti/Ni nanolaminates	in Ti	phase transformation and partial dislocations (FCC-Ti)	– 1/6⟨112⟩
		in Ni	full dislocations and multiple dislocations	1/2⟨110⟩ –
	pure Ti		phase transformation and partial dislocations (FCC-Ti)	– 1/6⟨112⟩
	pure Ni		full dislocations	1/2⟨110⟩
Z direction (perpendicular to the interface)	Ti/Ni nanolaminates	in Ti	slip bands grain reorientation and twinning	–
		in Ni	partial dislocations	1/6⟨112⟩
	pure Ti		slip bands grain reorientation and twinning	–
	pure Ni		partial dislocations and full dislocations	1/6⟨112⟩ 1/2⟨110⟩

Quantitatively measuring the crack propagation behaviors of the Ti/Ni nanolaminates, the variations of crack length with tensile strains for different models are obtained and shown in Fig. 9. Here, the crack length is calculated as the straight distance between the two crack tips. As the loading is applied along the *Y* direction, the crack length of the sample with the crack in Ni layer is larger than the other samples, and the full dislocations and subsequent multiple dislocations dominate the plastic behavior at the crack tip. While in the Z direction, the crack length of the sample with a crack in Ti layer is larger than the other samples, which deform mainly through deformation twinning after the grain has been reorientated. It can be inferred that the full dislocations and succedent multiple dislocations in FCC Ni and deformation twinning in HCP Ti sharpen the crack tip, which promotes the crack growth. However, partial dislocation emissions in FCC Ti or Ni blunt the crack, which is not conducive to the crack growth. The conclusions of the present work are slightly different from those in the Ref. [47]. They studied tensile behaviors of center-cracked Zr (HCP) and Nb (BCC) and concluded that full dislocations blunted the crack tip, while the twinning sharpened the crack tip and promoted the crack propagation. In the present paper, the full dislocations and multiple dislocations in FCC Ni and twinning in HCP Ti emitted from the crack tip can also promote the crack growth, and the partial dislocations in FCC Ni make the crack passivated. The difference may be ascribed to the joint action of full dislocations and multiple dislocations in the present work. Continuous emission of full dislocations from the crack tip causes the "step structure" to accumulate. Meanwhile, the subsequent multiple dislocations further sharpen the crack tip. The co-operation between full dislocations and multiple dislocations eventually accelerates the crack growth. However, dense stacking faults induced by the partial dislocations evolve from the crack tip eventually passivate the crack tip. In addition, it is also necessary to emphasize that the crack propagation of cracked Ti/Ni nanolaminates is larger than that of the pure model. This is related to the fact that dislocations generating from the interface move towards the crack tip and further sharpen the crack.

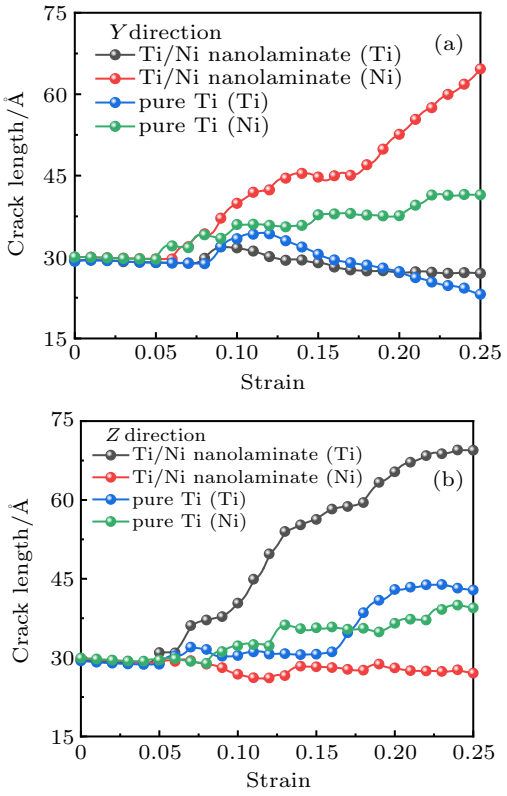


Fig. 9. Variations of crack length with tensile strains under different loading directions, showing tension loading applied along (a) *Y* and (b) *Z* directions, with brackets in the legend indicating crack at a certain internal layer.

Pre-existing crack significantly affects the mechanical properties and plastic deformation mechanism of nanostructured material. Generally, crack propagation in a nanostructured material is a complex problem. It is affected not only by the intrinsic crystallographic orientation of the sample and morphology of the crack tip, but also by extrinsic temperature and strain rate.[41,42,45,46] The attempt in the present work only focuses on the effects of loading direction and crystallographic orientation on the crack growth and deformation mechanism of Ti/Ni nanolaminate. Therefore, more efforts are needed to obtain more comprehensive deformation mechanism in cracked nano-laminated material.

4. Conclusions

In this paper, we investigate the effect of pre-existing crack on plastic deformation mechanism of Ti/Ni nanolaminate. The results demonstrate that the pre-existing crack significantly changes the plastic deformation mechanism of Ti/Ni nanolaminate. The plastic deformation transition of cracked Ti/Ni nanolaminate is ascribed to orientation-dependent tensile behaviors at the crack tip, which is due to the anisotropy of the certain crystal structure and loading direction. The main results of this paper are listed as follows.

(i) High stress concentration on the pre-existing crack causes the plastic deformation to occur first at the crack rather than the interface in cracked Ti/Ni nanolaminate, which dramatically reduces the strength of Ti/Ni nanolaminate.

(ii) Unlike the case of crack-free Ti/Ni nanolaminate, plastic deformation mechanism dramatically change with cracks either in Ti layer or in Ni layerin different loading directions. The interaction between the interfacial dislocations and different plastic deformation carriers initiated from the crack tip dominates the subsequent plastic deformation of the cracked Ti/Ni nanolaminate.

(iii) As the tension loading is applied parallel to the interface (Y direction), the main deformation behaviors of Ti/Ni nanolaminate with crack in Ti layer are phase transformation of HCP to FCC structure in Ti layer and partial dislocations gliding in Ni layer. As for the sample with the crack in Ni layer, full dislocations continually emitted from the crack tip in Ni layer, and phase transformation of HCP to FCC structure in Ti layer dominate the plastic behaviors of the cracked Ti/Ni nanolaminate. The Ti/Ni interface impedes the movement of the initial defects, but it can also serve as a dislocation source and sink in the tension process.

(iv) When the loading is applied perpendicularly to the interface (Z direction), the grain reorientation in Ti layer and dislocation propagation in Ni layer dominate the plastic deformation of Ti/Ni nanolaminate with crack in Ti layer. As for the sample with crack in Ni layer, continuous partial dislocations are emitted from the crack tip and glide along the adjacent planes, resulting in deformation twinning in Ni layer, and grain reorientation occurring in Ti layer. The interaction between the interface and defect arising from the crack tip also ensures good plastic properties of cracked Ti/Ni nanolaminate.

(v) Full dislocations and subsequent multiple dislocations in FCC structure and deformation twinning in HCP structure can easily trigger the crack growth, while the partial dislocations in the FCC structure blunt the crack. Besides, the interfacial dislocations moving towards the crack tip can further sharpen the crack in Ti/Ni nanolaminate.

References

[1] Kumar M S, B"oni P and Tixier S 1998 *Physica B* **248** 53
[2] Veres T, Cser L, Bodnarchuck V, Ignatovich V, Horvath Z E and Nagy B 2013 *Thin Solid Films* **540** 69
[3] Bhatt P, Ganeshan V, Reddy V R and Chaudhari S M 2006 *Appl. Surf. Sci.* **253** 2572
[4] Yang Z W, Lian J, Cai X Q, Wang Y, Wang D P and Liu Y C 2019 *Intermetallics* **109** 179
[5] Lehnert T, Grimmer H, Böni P, Horisberger M and Gotthardt R 2000 *Acta Mater.* **48** 4065
[6] Shi J, Wei M Z, Ma Y J, Xu L J, Cao Z H and Meng X K 2015 *Mater. Sci. Eng. A* **648** 31
[7] Shi J, Cao Z H and Zheng J G 2017 *Mater. Sci. Eng. A* **680** 210
[8] Yang Z and Wang J L 2015 *J. Appl. Mech.* **82** 011008
[9] Yang Z and Wang J L 2016 *J. Mech. Phys. Solids* **88** 72
[10] Wang C, Song H Y and An M R 2014 *Acta Phys. Sin.* **63** 046201 (in Chinese)
[11] Zhang G W, Yang Z L and Luo G 2016 *Chin. Phys. B* **25** 086203
[12] An M R, Song H Y and Su J F 2012 *Chin. Phys. B* **21** 106202
[13] Zhao B B, Wang Y, Liu C and Wang X C 2016 *Chin. Phys. B* **25** 114601
[14] Li R, Liu T, Chen X, Chen S C, Fu Y H and Liu L 2018 *Acta Phys. Sin.* **67** 190202 (in Chinese)
[15] Misra A and Krug H. 2001 *Adv. Eng. Mater.* **3** 217
[16] Hoagland R G, Kurtz R J and Henager Jr C H 2004 *Scripta Mater.* **50** 775
[17] Wang J, Zhou Q, Shao S and Misra A 2017 *Mater. Res. Lett.* **5** 1
[18] Zhou Q, Du Y, Ren Y, Kuang W W, Han W C, Wang H F, Huang P, Wang F and Wang J 2019 *J. Alloys Compd.* **776** 447
[19] Hua D P, Ye W T, Jia Q, Zhou Q, Xia Q S, Shi J Q, Deng Y Y and Wang H F 2020 *Appl. Surf. Sci.* **511** 145545
[20] Hoagland R G, Mitchell T E, Hirth J P and Kung H 2002 *Philos. Mag. A* **82** 643
[21] Imran M, Hussain F, Rashid M and Ahmad S A 2012 *Chin. Phys. B* **21** 126802
[22] Wang J, Hoagland R G, Hirth J P and Misra A 2008 *Acta Mater.* **56** 5685
[23] Zhang R F, Wang J, Beyerlein I J and Germann T C 2011 *Scripta Mater.* **65** 1022
[24] An M R, Song H Y, Deng Q, Su M J and Liu M Y 2019 *J. Appl. Phys.* **125** 165307
[25] Zhang J Y, Zhang X, Wang R H, Lei S Y, Zhang P, Niu J J, Liu G, Zhang G J and Sun J 2011 *Acta Mater.* **59** 7368
[26] Song H Y and Li Y L 2015 *Chin. Phys. B* **25** 026802
[27] Li Y, Zhou Q, Zhang S, Huang P, Xu K K and Wang F 2018 *Appl. Surf. Sci.* **433** 957
[28] Wadley H N G, Zhou X, Johnson R A and Neurock M 2001 *Prog. Mater. Sci.* **46** 329
[29] Zhou X W, Wadley H N G, Johnson R A, Larson D J, Tabat N, Cerezo A, Petford-long A K, Smith G D W, Clifton P H, Martens R L and Kelly T F 2001 *Acta Mater.* **49** 4005
[30] Fan Q, Xu J G, Song H Y and Zhang Y G 2015 *Acta Phys. Sin.* **64** 016201 (in Chinese)
[31] Yang M, Xu J G, Song H Y and Zhang Y G 2015 *Chin. Phys. B* **24** 096202
[32] Tian Y Y, Li J, Hu Z Y, Wang Z P and Fang Q H 2017 *Chin. Phys. B* **26** 126802
[33] Cheung K S and Yip S 1991 *J. Appl. Phys.* **70** 5688
[34] Stukowski A 2009 *Model. Simul. Mater. Sci. Eng.* **18** 015012
[35] Faken D and Jónsson H 1994 *Comp. Mater. Sci.* **2** 279
[36] Stukowski A, Bulatov V V and Arsenlis A *Model. Simul. Mater. Sci. Eng.* **20** 085007
[37] Ren J Q, Sun Q Y, Xiao L, Ding X D and Sun J 2014 *Comp. Mater. Sci.* **92** 8
[38] An M R, Deng Q, Li Y L, Song H Y, Su M J and Cai J 2017 *Mater. Des.* **127** 204
[39] Chen P, Wang F X and Li B 2019 *Acta Mater.* **171** 65
[40] An M R, Su M J, Deng Q, Song H Y, Wang C and Shang Y 2020 *Chin. Phys. B* **29** 046201
[41] Tang T, Kim S, Horstemeyer M F 2010 *Comp. Mater. Sci.* **48** 426
[42] Cai J, Mi C W, Deng Q and Zheng C Y 2019 *Mech. Mater.* **139** 103205
[43] Su M J, Deng Q, An M R, Liu L T, Ma C B 2019 *Comp. Mater. Sci.* **158** 149
[44] Hai S and Tadmor E B 2003 *Acta Mater.* **51** 117
[45] Warner D H and Curtin W A 2009 *Acta Mater.* **57** 4267
[46] Yamakov V I, Warner D H, Zamora R J, Saether E, Curtin W A and Glaessgen E H 2014 *J. Mech. Phys. Solids* **65** 35
[47] Singh D, Sharma P, Jindal S, Kumar P, Kumar P and Parashar A 2019 *Curr. Appl. Phys.* **19** 37